

A numerical model for charge transport and energy conversion of perovskite solar cells–SI

Yecheng Zhou* and Angus Gray-Weale

School of Chemistry, The University of Melbourne, Parkville, VIC, 3010, Australia

E-mail: zhouych87@gmail.com

*To whom correspondence should be addressed

Numerical solution process details

Adapted equations and boundary conditions

The specific method we used to solve our equations are the relaxation method for ‘Two Point Boundary Value Problems’ in *Numerical Recipes in Fortran*.¹ Here, for convenience, we repeat these five first differential equations:

$$\begin{aligned}
 J_p &= -eD_p \frac{\partial p}{\partial x} + ep\mu_p F; & J_n &= eD_n \frac{\partial n}{\partial x} + en\mu_n F \\
 \frac{\partial J_n}{\partial x} &= -eG + eR; & \frac{\partial J_p}{\partial x} &= eG - eR \\
 \frac{\partial F}{\partial x} &= e \frac{p - n}{\varepsilon \varepsilon_0}
 \end{aligned} \tag{1}$$

and five boundary conductions:

$$\begin{aligned}
 J_n|_{x=d} &= 0; & J_p|_{x=0} &= 0; & F_{x=0} &= F_0 \\
 F_{x=d} &= F_d; & n|_{x=0}p|_{x=d} &= N_c N_v e^{\frac{E_{bgap} - V}{-kT}}
 \end{aligned} \tag{2}$$

If we want to use the ‘Two point Boundary Value Problems’ method in *Numerical Recipes in Fortran*,¹ all of the equation must be the first order differential and the boundary condition at two point is not coupled. While, the last boundary condition in Equation 2 is coupled. To decouple we add a new function $n^0(x) = n|_{x=0}$, which is the electron density at $x=0$. It is a constant. To simplify, we set $J_n = J_n/e, J_p = J_p/e, n = ne$ and $p = pe$. We rewrite Equations 1 in the form used in *Numerical Recipes in Fortran* ($\frac{\partial y}{\partial x} = g(x, y)$):

$$\begin{aligned}
 \frac{\partial p}{\partial x} &= (p\mu_p F - J_p)/D_p; & \frac{\partial n}{\partial x} &= (J_n - n\mu_n F)/D_n \\
 \frac{\partial J_n}{\partial x} &= -G + R; & \frac{\partial J_p}{\partial x} &= G - R \\
 \frac{\partial F}{\partial x} &= \frac{p - n}{\varepsilon \varepsilon_0}; & \frac{\partial n^0}{\partial x} &= 0
 \end{aligned} \tag{3}$$

and boundary conditions:

$$\begin{aligned}
J_p|_{x=0} &= 0; & F|_{x=0} &= F_0; & n|_{x=0} &= n^0|_{x=0} \\
F|_{x=d} &= F_d; & J_n|_{x=d} &= 0; & p|_{x=d} &= \frac{N_c N_v}{n^0|_{x=d}} e^{\frac{E_{\text{bandgap}} - V}{-kT}}
\end{aligned} \tag{4}$$

To implement these six (total number of equations, noted as N in *Numerical recipes*) equations into Fortran code, differential Equations 3 are approximated by *finite-difference equations* (FDEs) on a grid of points (total point number, noted as M in *Numerical recipes*, we will discuss it in section **Mesh test**) that spans whole perovskite layer:

$$\begin{aligned}
n^0(k) - n^0(k-1) &= 0 \\
J_p(k) - J_p(k-1) - h(G - R) &= 0 \\
F(k) - F(k-1) - h\left(\frac{\frac{p(k)+p(k-1)}{2} - \frac{n(k)+n(k-1)}{2}}{\varepsilon\varepsilon_0}\right) &= 0 \\
n(k) - n(k-1) - h\left(\frac{J_n(k) + J_n(k-1)}{2D_n} - \frac{\mu_n}{D_n} \frac{n(k) + n(k-1)}{2} \frac{F(k) + F(k-1)}{2}\right) &= 0 \\
p(k) - p(k-1) - h\left(\frac{\mu_p}{D_p} \frac{p(k) + p(k-1)}{2} \frac{F(k) + F(k-1)}{2} - \frac{J_p(k) + J_p(k-1)}{2D_p}\right) &= 0 \\
J_n(k) - J_n(k-1) - h(-G + R) &= 0
\end{aligned} \tag{5}$$

where $h = x(k) - x(k-1)$. Then the problem becomes FDEs on a mesh of M points, a solution consists of values for N dependent functions given at each of the M mesh points, or $N \times M$ variables in all. The method determines the solution by starting with a guess and improving it, iteratively. As the iterations improve the solution, the result is said to relax to the true solution.

General procedures

To simplify illustration, we set all these parameters as: $y_1 = n^0$; $y_2 = J_p$; $y_3 = F$; $y_4 = n$; $y_5 = p$; $y_6 = J_n$. We use the notation \mathbf{y}_k to refer the entire set of dependent variables y_1, y_2, \dots, y_6 at point x_k , and use the notation \mathbf{g}_k to refer all the functions. Then Equation 5

can be written:

$$0 = \mathbf{E}_k \equiv \mathbf{y}_k - \mathbf{y}_{k-1} - (x_k - x_{k-1})\mathbf{g}_k(x_k, x_{k-1}, \mathbf{y}_k, \mathbf{y}_{k-1}) \quad (6)$$

Where \mathbf{E}_k is the errors of guessed solution. Equation 6 provides six equations coupling twelve variables at point $k, k - 1$. There are $M - 1$ points, $k = 2, 3, \dots, M$. Thus, Equation 6 provides a total of $(M - 1)N$ equations for $6M$ unknowns. The remaining six equations come from boundary conditions.

At the first boundary ($x = 0$), we have 3 conditions (first three in Equation 4)

$$0 = \mathbf{E}_1 \equiv \mathbf{B}(\mathbf{x}_1, \mathbf{y}_1) \quad (7)$$

while at the second boundary ($x = d$, last three in Equation 4)

$$0 = \mathbf{E}_{M+1} \equiv \mathbf{C}(\mathbf{x}_M, \mathbf{y}_M) \quad (8)$$

The solution of Equation 6, 7 and 8 consist of the six variables y_j at the M points x_k . We give a **initial guess** (we will give it later), then corrections was applied to approximating to the solution. The correction are developed by expanding the FDEs in first-order Taylor series with respect to small changes $\Delta\mathbf{y}$. At an interior point ($2 < k < M$), this gives:

$$\mathbf{E}_k(\mathbf{y}_k + \Delta\mathbf{y}_k, \mathbf{y}_{k-1} + \Delta\mathbf{y}_{k-1}) \approx \mathbf{E}_k(\mathbf{y}_k, \mathbf{y}_{k-1}) + \sum_{i=1}^N \frac{\partial \mathbf{E}_k}{\partial y_{i,k-1}} \Delta y_{i,k-1} + \sum_{i=1}^N \frac{\partial \mathbf{E}_k}{\partial y_{i,k}} \Delta y_{i,k} \quad (9)$$

To approach a solution, $\mathbf{E}(\mathbf{y} + \Delta\mathbf{y})$ should be updated to be zero. The general set of equations at an interior point can be written in matrix form as

$$\sum_{i=1}^6 S_{j,i} \Delta y_{i,k-1} + \sum_{i=6+1}^{12} S_{j,i} \Delta y_{i-6,k} = -E_{j,k}, \quad j = 1, 2, \dots, 6 \quad (10)$$

where, $S_{j,i} = \frac{\partial \mathbf{E}_k}{\partial y_{i,k-1}}$, $S_{j,i+6} = \frac{\partial \mathbf{E}_k}{\partial y_{i,k}}$. The dimension of $S_{j,i}$ is 6×12 at each k .



Figure 1: Matrix structure of a set of linear six FDEs with three boundary conditions imposed at both endpoints. One X represents a coefficient of the FDEs, V represents a component of the unknown solution vector, and B is a component of the known right-hand side. Empty spaces represent zeros.

Similarly, the algebraic relations at the boundaries can be expanded in a first-order Taylor series for increments that improve the solution. Since \mathbf{E}_1 depends only on \mathbf{y}_1 , we find at the first boundary:

$$\sum_{i=1}^6 S_{j,i} \Delta y_{i,1} = -E_{j,1}, \quad j = 4, 5, 6 \quad (11)$$

where $S_{j,i} = \frac{\partial E_{j,1}}{\partial y_{n,1}}$. At the second boundary,

$$\sum_{i=1}^6 S_{j,i} \Delta y_{i,M} = -E_{j,M+1}, \quad j = 1, 2, 3 \quad (12)$$

where $S_{j,i} = \frac{\partial E_{j,M+1}}{\partial y_{n,M}}$.

We thus have in Equations 10, 11 and 12 a set of linear equations to be solved for the correction $\Delta \mathbf{y}$, iterating until the corrections are sufficiently small. The equations have a

special structure, because each $S_{j,i}$ couples only points $k, k-1$. Figure 1 shows the structure of the complete matrix equation for the case of $M = 3$. There are 3 boundary conditions at the first and at the second boundary. The block boxed by red lines at left-up corner comes from the boundary condition $S_{j,i}$ at point $k = 1$. Next two are the $S_{j,i}$ from $k = 2$ and $k = 3$. The last block is corresponding to the 3 second boundary conditions. This special form matrix is diagonalized by splitting into it M small matrix, and then diagonalize the matrix from the first point $k = 1$ to the last points $k = M + 1$. For more details, please check *Numerical recipes*.

S matrix

S matrix varies for different models. Here, we use direct recombination model ($R = r \times n \times p$, Equation 12 in main text) as an example. For SRH model and other models, the $S_{j,i}$ at each k points can be obtained by its definition in Equation 6, 7 and 8. To simplify illustration, we set all these parameters as: $y_1 = n^0$; $y_2 = J_p$; $y_3 = F$; $y_4 = n$; $y_5 = p$; $y_6 = J_n$. Here, we only shows non-zero element. h is the size of discretion, $h = x(k) - x(k-1) = \frac{d}{M}$. We substitute μ with Einstein relation $\mu = \frac{eD}{kT} = \frac{D}{0.026}$ and R with $rn p$. Equation 5 can be rewritten:

$$\begin{aligned}
y_1(k) - y_1(k-1) &\equiv E_1 = 0 \\
y_2(k) - y_2(k-1) - h(G - r \frac{y_5(k) + y_5(k-1)}{2} \frac{y_4(k) + y_4(k-1)}{2}) &\equiv E_2 = 0 \\
y_3(k) - y_3(k-1) - h(\frac{\frac{y_5(k)+y_5(k-1)}{2} - \frac{y_4(k)+y_4(k-1)}{2}}{\varepsilon \varepsilon_0}) &\equiv E_3 = 0 \\
y_4(k) - y_4(k-1) - h(\frac{y_6(k) + y_6(k-1)}{2D_p} - \frac{\mu_p}{D_p} \frac{y_4(k) + y_4(k-1)}{2} \frac{y_3(k) + y_3(k-1)}{2}) &\equiv E_4 = 0 \\
y_5(k) - y_5(k-1) - h(-\frac{y_2(k) + y_2(k-1)}{2D_n} + \frac{\mu_n}{D_n} \frac{y_5(k) + y_5(k-1)}{2} \frac{y_3(k) + y_3(k-1)}{2}) &\equiv E_5 = 0 \\
y_6(k) - y_6(k-1) - h(-G + r \frac{y_5(k) + y_5(k-1)}{2} \frac{y_4(k) + y_4(k-1)}{2}) &\equiv E_6 = 0
\end{aligned} \tag{13}$$

For convenience's sake, we define $tmp1 = y(4, k) + y(4, k - 1)$; $tmp2 = y(5, k) + y(5, k - 1)$; $tmp = tmp1 + tmp2$. The S matrix is shown below written in Fortran. Here, LT is the recombination coefficient r , ne is six (the number of equation, noted as N in *Numerical recipes*). S(i,jsf) is the last element for calculating E , then jsf= $2N + 1$.

For interior points $k = 2, 3, \dots, M$

$$s(1,1)=-1; \quad s(1,ne+1)=1; \quad s(1,jsf)=y(1,k)-y(1,k-1)$$

$$s(2,4)=0.25*h*tmp2*LT; \quad s(2,ne+4)=s(2,4); \quad s(2,5)=0.25*h*tmp1*LT$$

$$s(2,ne+5)=s(2,5); \quad s(2,2)=-1.0; \quad s(2,ne+2)=1.0$$

$$s(2,jsf)=y(2,k)-y(2,k-1)+h*((0.25*tmp1*tmp2*LT-ni*ni)-g)$$

$$s(3,4)=0.5*h/(\varepsilon\varepsilon_0); \quad s(3,ne+4)=s(3,4)$$

$$s(3,5)=-0.5*h/(\varepsilon\varepsilon_0); \quad s(3,ne+5)=s(3,5)$$

$$s(3,3)=-1.0; \quad s(3,ne+3)=1.0$$

$$s(3,jsf)=y(3,k)-y(3,k-1)-0.5*h*(tmp2-tmp1)/(\varepsilon\varepsilon_0)$$

$$s(4,4)=-1.+h*(y(3,k)+y(3,k-1))/(4*kt); \quad s(4,6)=-.5*h/de$$

$$s(4,ne+4)=1.+h*(y(3,k)+y(3,k-1))/(4*kt); \quad s(4,ne+6)=-.5*h/de$$

$$s(4,3)=h*tmp1/(4*kt); \quad s(4,ne+3)=h*tmp1/(4*kt)$$

$$s(4,jsf)=y(4,k)-y(4,k-1)-0.5*h*((y(6,k)+y(6,k-1))/de-tmp1*(y(3,k)+y(3,k-1))/(2*kt))$$

$$s(5,5)=-1.-h*(y(3,k)+y(3,k-1))/(4*kt); \quad s(5,2)=0.5*h/dh$$

$$s(5,ne+5)=1.-h*(y(3,k)+y(3,k-1))/(4*kt); \quad s(5,ne+2)=0.5*h/dh$$

$$s(5,3)=-h*tmp2/(4*kt); \quad s(5,ne+3)=-h*tmp2/(4*kt)$$

$$s(5,jsf)=y(5,k)-y(5,k-1)+0.5*h*((y(2,k)+y(2,k-1))/dh-tmp2*(y(3,k)+y(3,k-1))/(2*kt))$$

$$s(6,6)=-1.0; \quad s(6,ne+6)=1.0$$

$$\begin{aligned}
s(6,4) &= -0.25 * h * tmp2 * LT; & s(6,ne+4) &= s(6,4) \\
s(6,5) &= -0.25 * h * tmp1 * LT; & s(6,ne+5) &= s(6,5) \\
s(6,j\text{sf}) &= y(6,k) - y(6,k-1) - h * ((0.25 * tmp1 * tmp2 * LT - ni * ni) - g)
\end{aligned}$$

At the first boundary(x=0, k=1)

$$\begin{aligned}
s(4,ne+3) &= 1.0; & s(5,ne+2) &= 1.0 \\
s(6,ne+4) &= 1.0; & s(6,ne+1) &= -1.0 \\
s(4,j\text{sf}) &= y(3,1) - E0; & s(5,j\text{sf}) &= y(2,1); & s(6,j\text{sf}) &= y(4,1) - y(1,1)
\end{aligned}$$

At the second boundary(x=d, k=M)

$$\begin{aligned}
s(1,ne+3) &= 1.0; & s(2,ne+6) &= 1.0; & s(3,ne+5) &= 1.0 \\
s(3,ne+1) &= \exp(v/(kt)) * n0 * n0 / (y(1,m) * y(1,m)) \\
s(1,j\text{sf}) &= y(3,m) - Ed; & s(2,j\text{sf}) &= y(6,m) \\
s(3,j\text{sf}) &= y(5,m) - \exp(v/(kt)) * n0 * n0 / y(1,m)
\end{aligned}$$

Initial Guess

In our model, the applied voltage (V) is implemented as one boundary condition. The current density is obtained from solution. We start with $V = 0V$, giving a initial guess, solving equations. Then, the solution of $V = 0V$ will be used as the initial guess solution under applied voltage $V = 10mV$. We increase the voltage with increment of 10 mV, until The desired voltage reached. The first initial guess are shown as below, where D is the thickness of perovskite layer. $myE0 = V/D$.

The first initial guess

do k=1,M

x(k)=(k-1)*h

y(1,k)=n0*exp(v/(2*kt))

y(2,k)=0.01*x(k)/D


```

y(3,k)=myE0
y(4,k)=n0*exp(v/(2*kt))*EXP(x(k)/D)
y(5,k)=n0*exp(v/(2*kt))*EXP(1-x(k)/D)
y(6,k)=(D-x(k))*0.01/D
end do

```

Error calculation and converged criteria

The total error is calculated by

$$Error = \frac{1}{6M} \sum_{k=1}^M \sum_{j=1}^6 \frac{|\Delta y(j, k)|}{scalv(j)} \quad (14)$$

Where $scalv(j)$ is the scale of variable $y(j)$. In *Numerical recipes*, the $scalv$ vector is defined by a constant vector. In this numerical model, charge densities are in the scale of 10^{10} to 10^{18} . If we define its $scalv$ as a constant, the error should in a very wide range. Therefore, we set $scalv(j)$ as the maximum value of previous $y(j, k)$. The convergence criteria ($conv$) is 1.0^{-20} . When error is smaller than $conv$, the solution was reached.

Charges densities, electric field and currents in perovskite solar cells

Mesh test

Here, we are going to test how many discretion points (M) are enough for our model. Models with and without interface recombination are carried out. As shown in Figure 5, for model without interface recombination, 801 points is enough to get a accurate solution. For the sake of safety, we set $M = 3001$ for model without interface recombinations. While, for the model with interface, more points are needed. We performed more test with an interface recombination with 2nm thickness and 1 ns charge carriers lifetime. It is found that there is

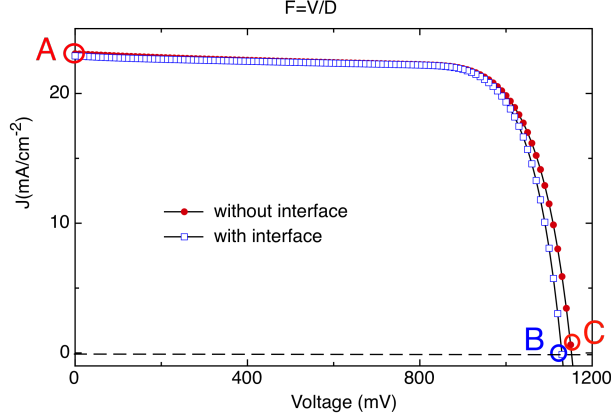


Figure 2: I-V charater curve simulated with boundary fields are $F(x = 0) = F(x = d) = V/d$. Other parameters are shown in manuscripts Table 1. Charges densities, currents and field at A, B and C points are shown in Figure 3.

no much difference between the solutions solved with $M = 20001$ and $M = 300001$. As the computation time is about proportional to M points, high density points needs long time. Therefore, we choose $M = 20001$ for models with interface recombination for time-saving.

Table 1: Parameters for M test.

α	Absorption coefficient	$5.7 \times 10^4 \text{cm}^{-1}$. ²	T	Temperature	300 K
$IPCE$	IPCE	100 %	I_l	Light intensity	1.5 AM
N_c, N_v	Density of States	$3.97 \times 10^{18} \text{cm}^{-3}$. ³	B_{gap}	Band gap	1.55 eV ⁴
D_n	Electron diffusion coefficient	$0.017 \text{cm}^2 \text{s}^{-1}$. ⁵	τ	Lifetime	736 ns ⁴
D_p	Hole diffusion coefficient	$0.011 \text{cm}^2 \text{s}^{-1}$. ⁵	F_0, F_d	Field at boundary	$\frac{V}{d}$
d	Perovskite thickness	350 nm ⁴	τ_{intf}	Interface Lifetime	1 ns

Parallelization

With a given V , J is determined by solving Equation 3. Every solution only give one point in J-V curve of a solar cell. On the other hand, the mesh points need to be large in order to achieve accurate solutions. Hence, to draw a J-V curve of a solar cell, it is time-consuming. Here, we implement MPI into our code for parallel calculation. The solution matrix is

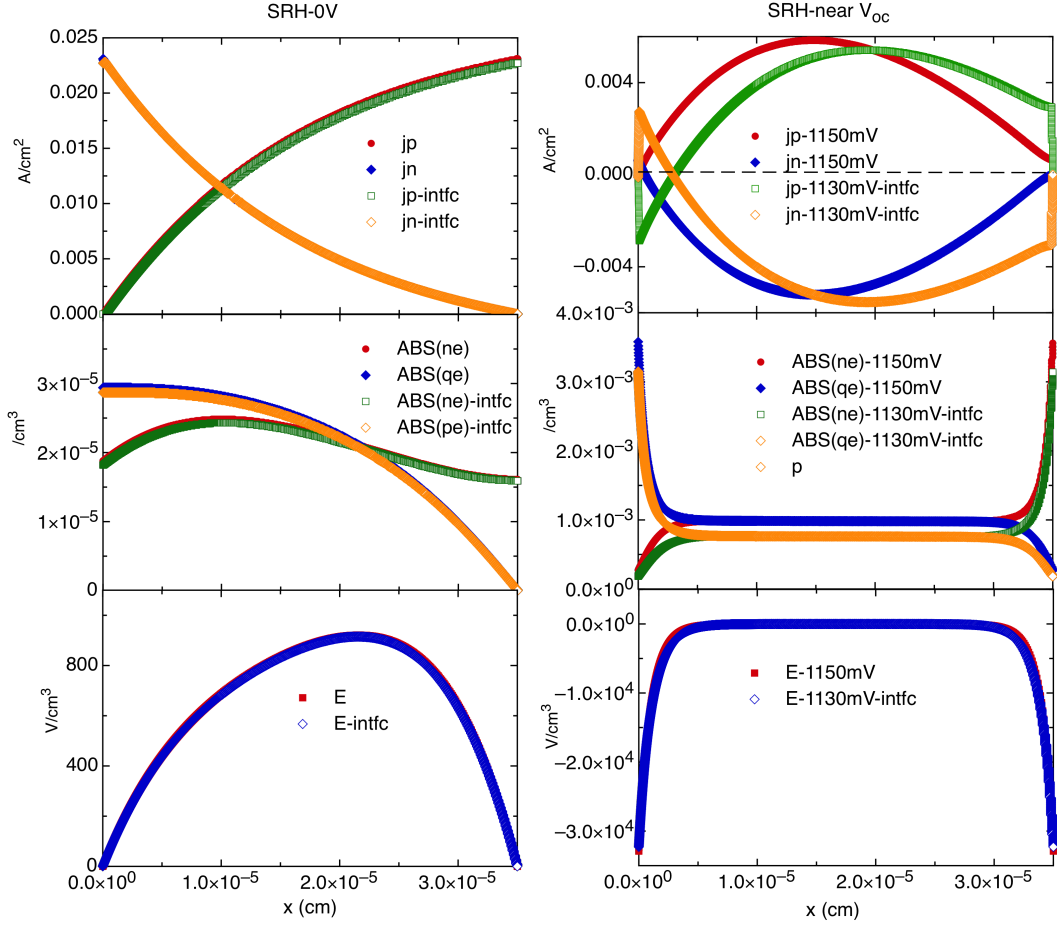


Figure 3: Simulated charges densities, electric fields and currents in perovskite solar cells. Left shows parameters at short circuit, point A in figure 2. Right shows parameters near open circuit, point B and C in figure 2. Boundary fields are $F(x = 0) = F(x = d) = V/d$. Other parameters are shown in manuscripts Table 1. The enlarged current distribution near TiO_2 side is shown in Figure 4.

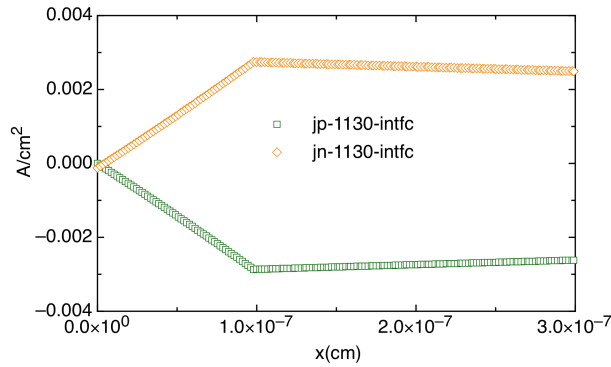


Figure 4: Currents near TiO_2 side in perovskite solar cells near open circuit simulated with interfaces. Boundary fields are $F(x = 0) = F(x = d) = V/d$. Other parameters are shown in manuscripts Table 1.

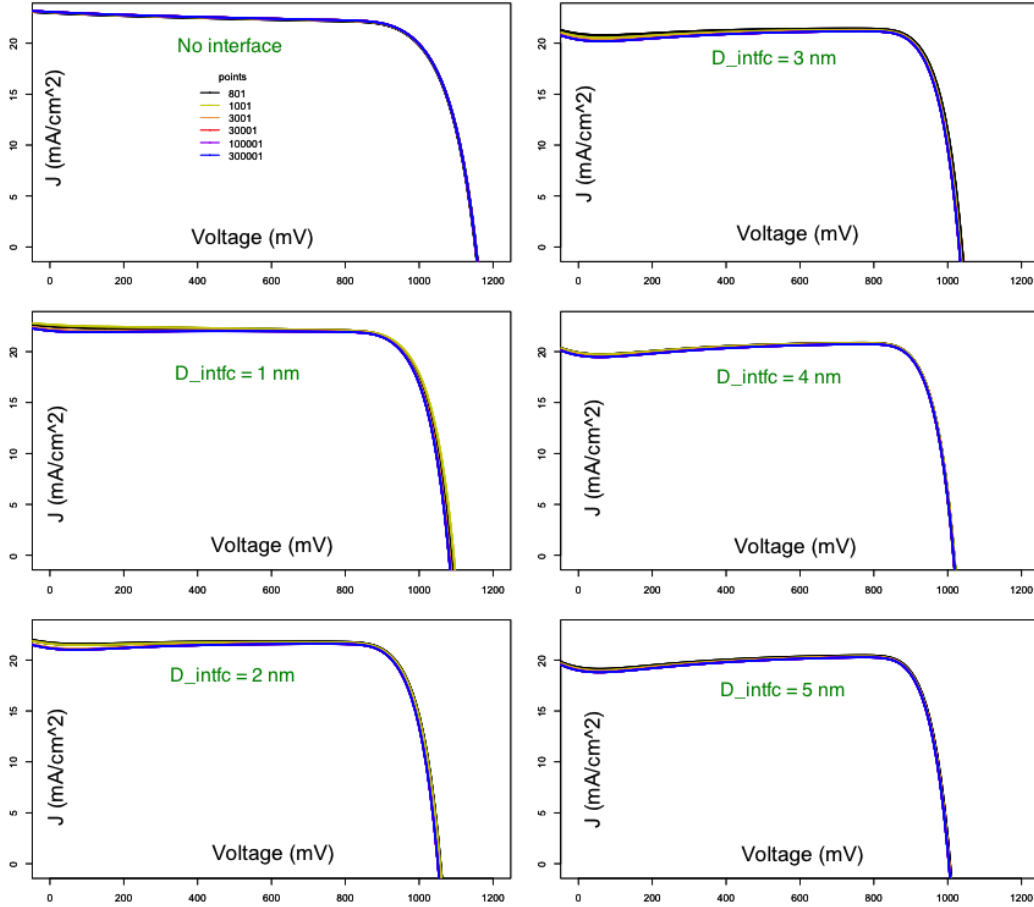


Figure 5: I-V curves of a solar cell with different number of mesh points and interface recombination thickness. In the interface recombination region, charge carrier's lifetime is set as 1 ns. More parameters are shown in Table 1

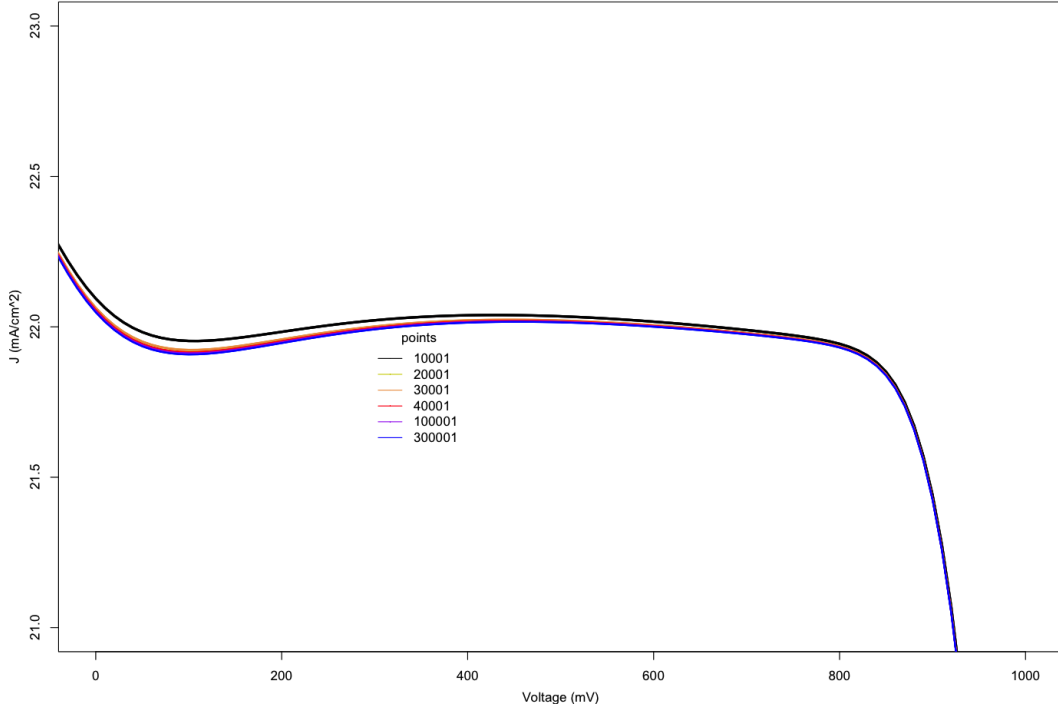


Figure 6: I-V curves of a solar cell with different number of mech. The interface recombination thickness is 2 nm. More parameters are shown in Table 1

diagonalised by splitting it into $M \times 6 \times 13$ submatrixs and diagonalising the submatrix from $k = 1$ to $k = M$. It is not wise to divide this process into several parts and to diagonalise on separated CPUs. Therefore, we scatter all of the V array to every CPU, and then solve them separately. Lastly, all of the solutions are collected by `MPI_GATHERV` function.

Lifetime dependence:

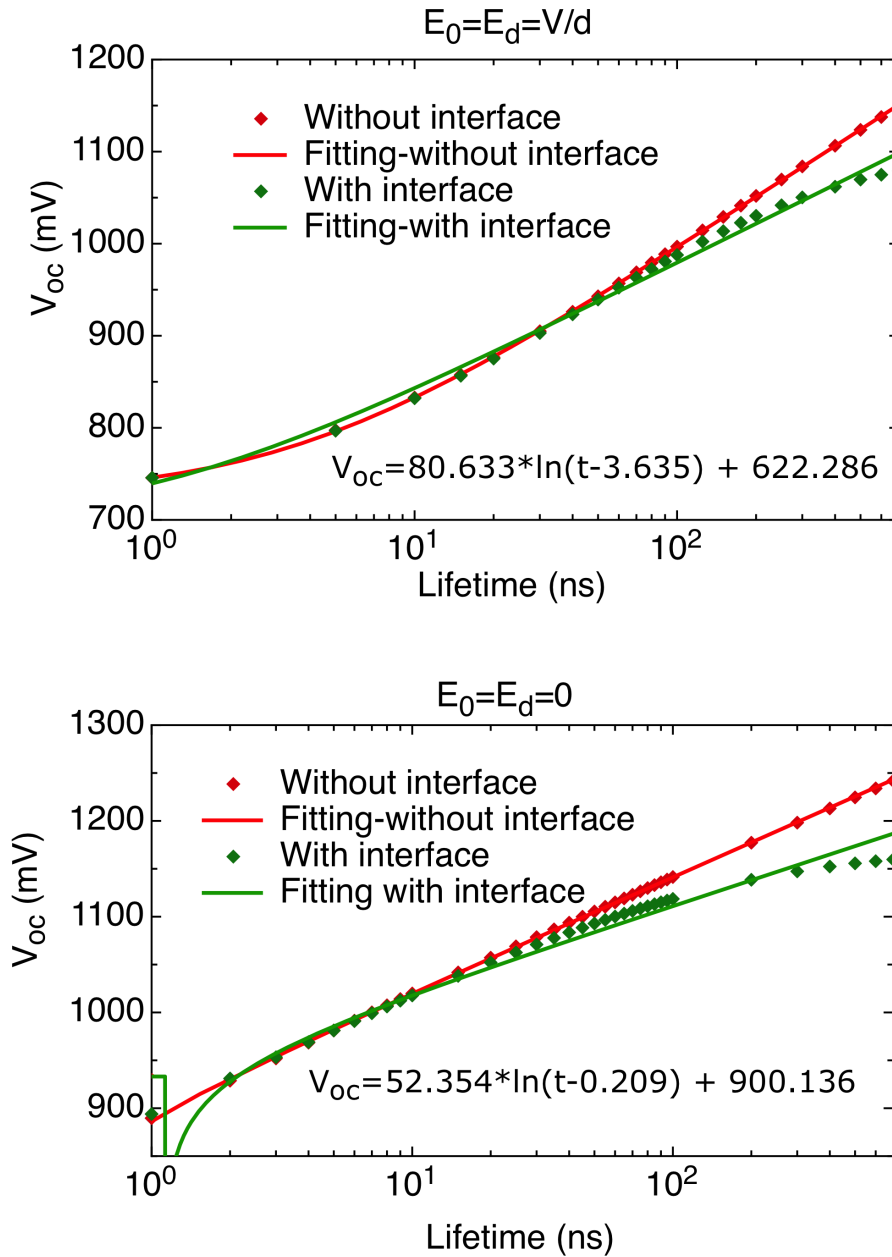


Figure 7: Lifetime depends V_{oc} with various lifetimes.

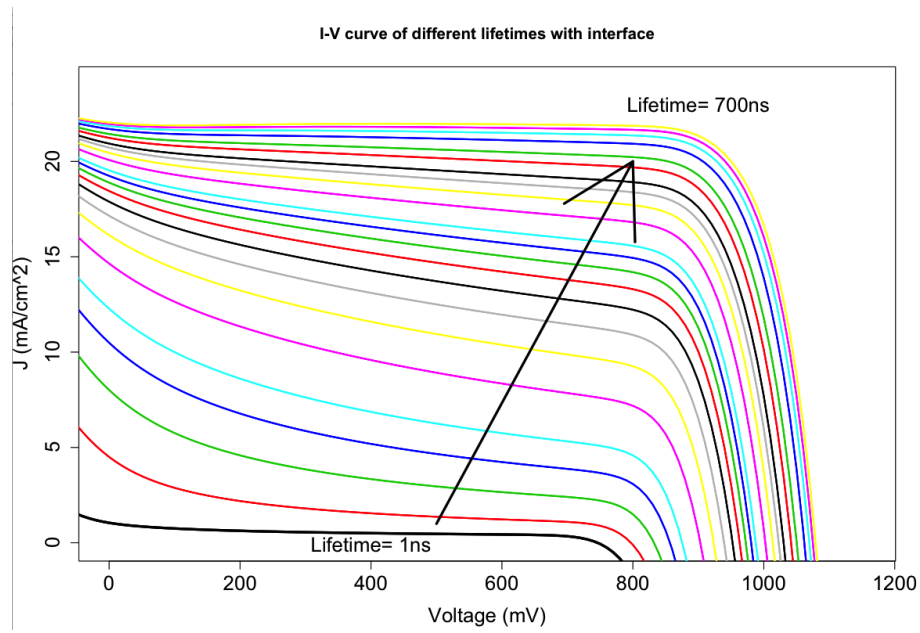


Figure 8: Solar cell's performance with various lifetimes with interface recombination.
 $F_0 = F_d = V_0/d$.

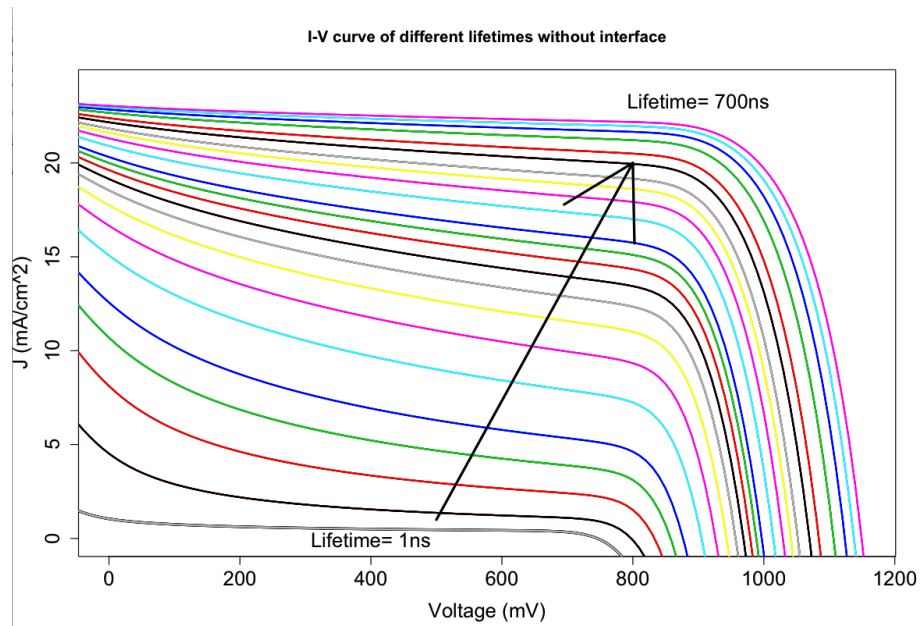


Figure 9: Solar cell's performance with various lifetimes without interface recombination.
 $F_0 = F_d = V_0/d$.

Mobility dependence:

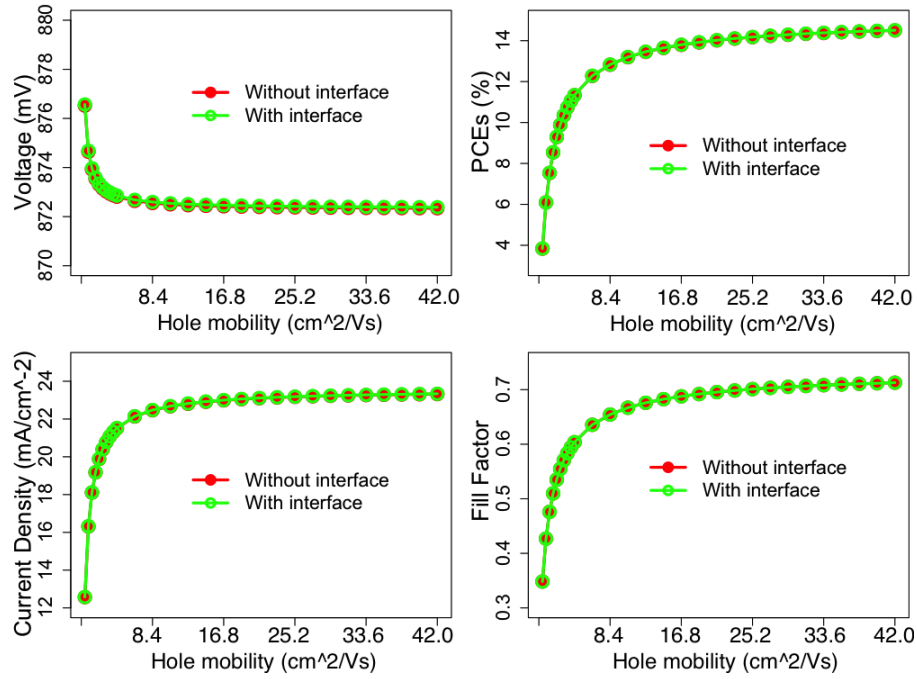


Figure 10: Solar cell's performance with mobilities. Both of the electron and hole mobilities increase at the same to certain times of 0.65(electron) and 0.42 (hole) cm^2/Vs , corresponding to diffusion coefficient of $0.017cm^2/s$ and $0.011cm^2/s$. $F_0=F_d=V_0/d$.

Temperature dependence:

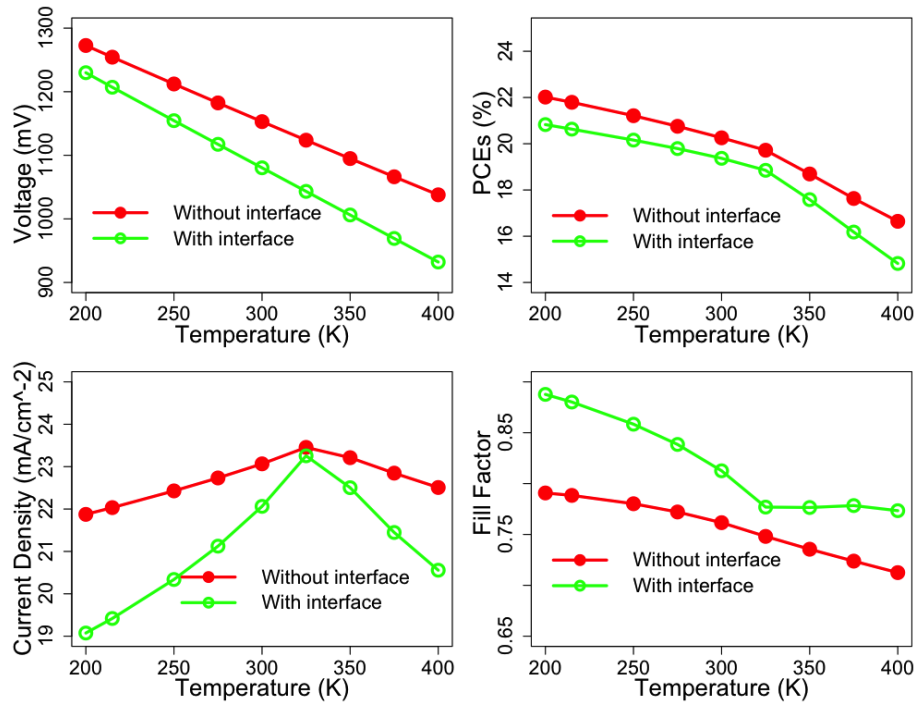


Figure 11: Temperature dependence with diffusion coefficients change. The thickness of simulated solar cell is 350 nm. The band gap is 1.55 eV. The interface recombination width is 5 nm and its lifetime is 5 ns. The lifetime in cell is assumed to be 736 ns. The cells work under 1 sun (1.5AM).

Thickness depends performance

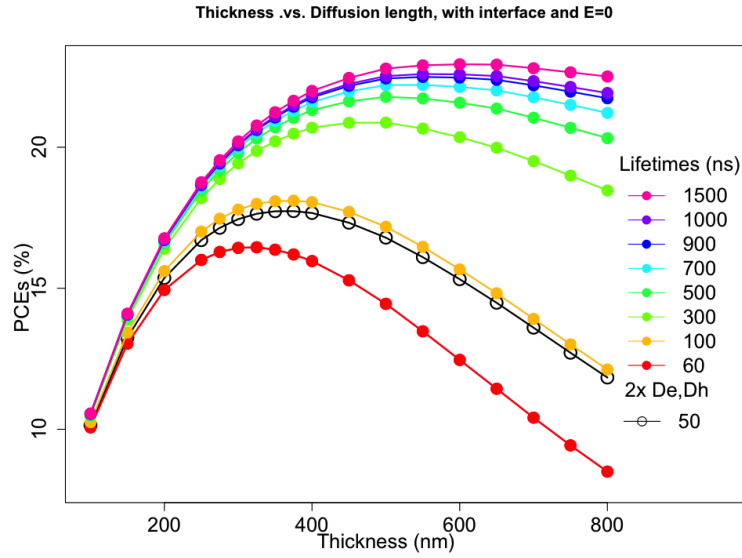


Figure 12: The thickness dependence PCEs. The optimum thickness is depended on the diffusion length. Modeled with interface. $F_0 = F_d = 0$

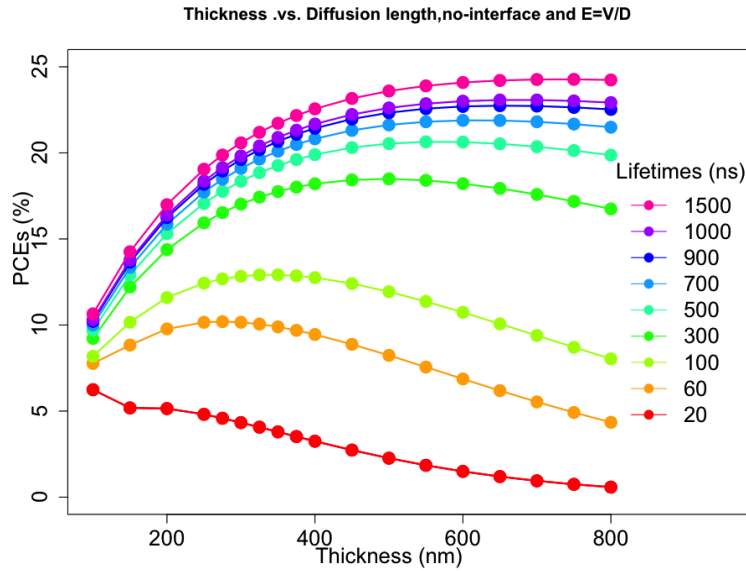


Figure 13: The thickness dependence PCEs. The optimum thickness is depended on the diffusion length. Modeled without interface. $F_0 = F_d = V/d$

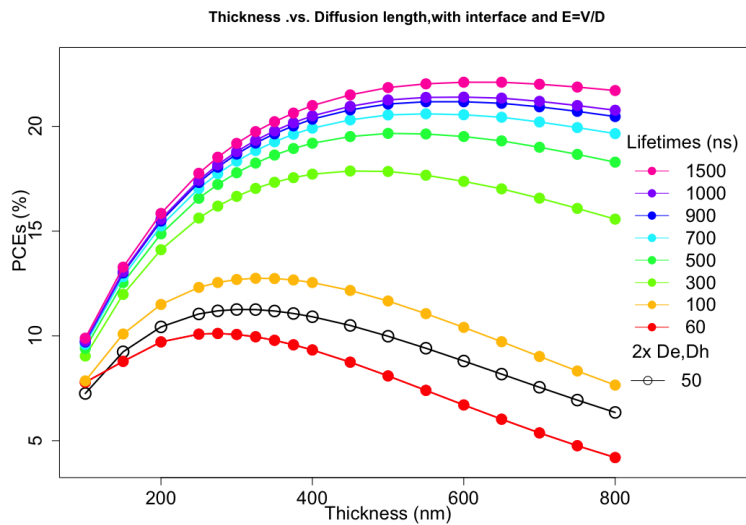


Figure 14: The thickness dependence PCEs. The optimum thickness is depended on the diffusion length. Modeled with interface. $F_0 = F_d = V/d$

Structure optimization

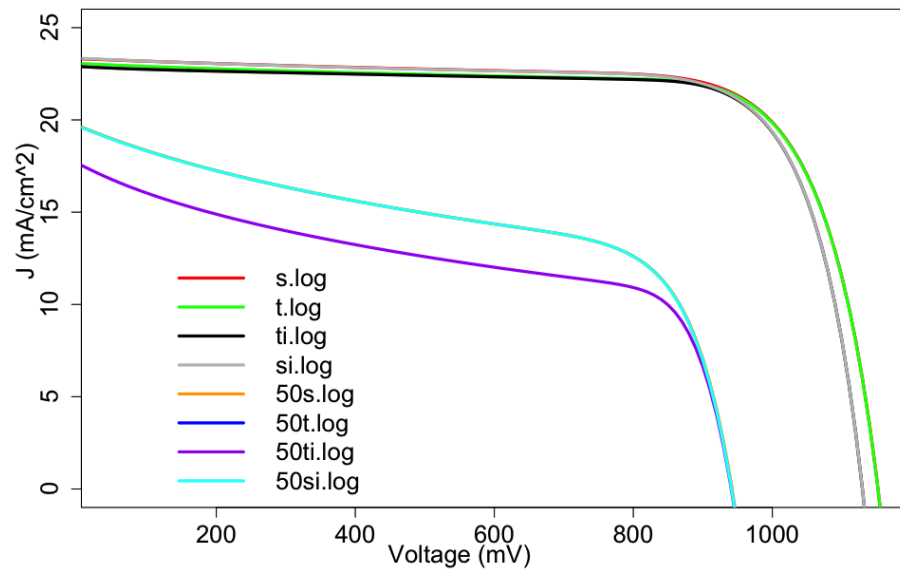


Figure 15: Models comparison of T and S model with or without interface, with life time of 736 ns or 50 ns. $F_{x=0} = F_{x=d} = \frac{V}{d}$

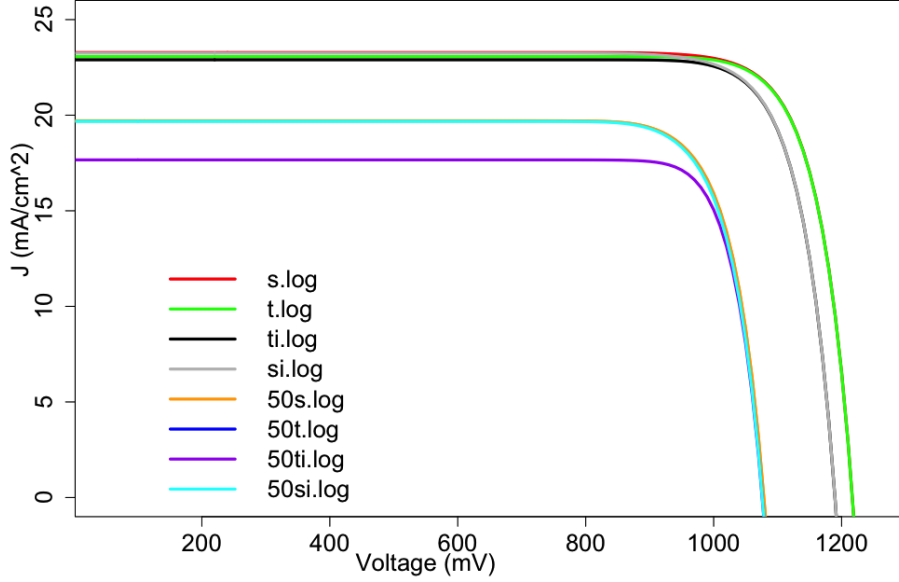


Figure 16: Models comparison of T and S model with or without interface, with life time of 736 ns or 50 ns. $F_{x=0} = F_{x=d} = 0$

Recombination coefficient estimation

As we have illustrated before that Equation 14 is the charge carriers lifetime deduce from Equation 12 under small charge injection under illumination.^{6,7} While in real case, the condition of small injection is not satisfied. But in experiment only lifetime of the charge carriers are available. Hence, we need to deduce the recombination coefficient from lifetime. The lifetime is measure as:^{2,5} They give a short time pulse illumination and then remove it, and measure the charge density. Their process is shown in figure 17. At first, the cell is irradiated by a pulse, during this period time photon generate charge carriers are become more and more until the charge density are saturated. Then remove the pulse, the charge density decrease with time past. After a lifetime period, the charge density become the $\frac{n_0}{e}$. Here, we will give the accurate relationship between the lifetime and recombination rate. In experiment, because there is no charge movement and no dopant in perovskite materials, hence, the electron density should be the same with hole density ($n = p$). Then charge

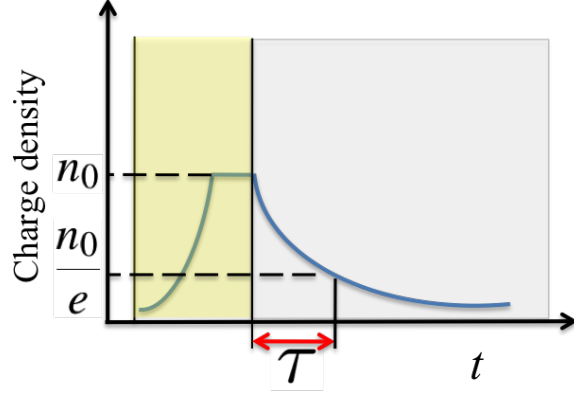


Figure 17: Measurement of lifetime: In the yellow shadow region, the cell is irradiated by the pulse, in this region photon generate charge carriers are become more and more until the charge density are saturated. Gray shadow covered region means the irradiation have been removed, the charge density decrease with time past.

carriers recombination rate can be expressed as

$$\frac{dn}{dt} = -R = -r \times n \times p = -rn^2$$

then we have:

$$n = \frac{1}{r(t - c)}$$

The measurement process is shown in figure 17. If the charge density dynamics in solar cell have reached a balance before illumination pulse removal. We define the time when pulse remove is zero. At $t = 0$, the charge density is n_0 , then we can get $c = \frac{-1}{rn_0}$. Hence:

$$n = \frac{n_0}{rn_0t + 1} \quad (15)$$

Uniformly distributed charge density

After the pulse removed, if the charge density in the device is uniformly distributed, at time τ , the charge density become $n = \frac{n_0}{e} = \frac{n_0}{rn_0\tau + 1}$. Therefore, the lifetime can be expressed as:

$$\tau = \frac{e - 1}{rn_0} \quad (16)$$

That's to say the charge carriers lifetime is depend on the initial charge density rather than a certain value. Larger charge density will lead to a short lifetime. If the charge density have reached a balance before measure the lifetime, the charge generation rate should be equal to the recombination rate: $G/d = r \times n_0^2$. Combining with equation (16), we can get

$$n_0 = \frac{G\tau}{L(e-1)} \quad (17)$$

Also we can know the recombination coefficient:

$$r = \frac{L(e-1)^2}{G\tau^2} = 3.51499 \times 10^{-6} \text{ cm}^3/\text{s} \quad (18)$$

Those calculations is based on the assumption that carriers lifetime is 736 ns and charges are generated uniformly.

Estimation of the initial light intensity at $x = 0$

Before the pulse remove, the total generated carriers should be the same with the total recombined carriers. Hence:

$$\int_0^d \frac{I_0}{L} e^{-x/L} dx = \int_0^d r n_0^2 e^{-2x/L} dx$$

$$I_0 \left(1 - e^{-\frac{d}{L}}\right) = \frac{1}{2} L n_0^2 r \left(1 - e^{-\frac{2d}{L}}\right)$$

We get:

$$n_0 = \sqrt{\frac{2I_0(e^{-\frac{d}{L}} - 1)}{Lr(e^{-\frac{2d}{L}} - 1)}}$$

$$= \sqrt{\frac{2I_0}{Lr(e^{-\frac{d}{L}} + 1)}}$$

Decay exponentially-1

For a more accurate case, the charge density near the light surface is much higher than the charge density inside thin film. This high density will play a very important role in the process of recombination. If the generate rate is exponential decay, the lifetime get more complicated. As the charge recombination is too fast for charge transport. Based on Equation 16, the lifetime at x is

$$\tau(x) = \frac{e - 1}{rn_x} \quad (19)$$

Where $n_x = n_0 e^{-\frac{x}{L}}$, L is the decay depth. n_0 is the initial light intensity at $x = 0$. It will be estimated later. The charge density at x and time t is $n(x, t) = n_0 e^{-\frac{x}{L}} \times e^{-\frac{t}{\tau(x)}}$. Then the lifetime measured in experiment is the time make below equation true:

$$\frac{\int_0^d n_0 e^{-\frac{x}{L}} \times e^{-\frac{t}{\tau(x)}} dx}{\int_0^d n_0 e^{-\frac{x}{L}} dx} = \frac{1}{e} \quad (20)$$

We get,

$$\frac{(e - 1) \left(e^{-\frac{rn_0 t e^{-\frac{d}{L}}}{e-1}} - e^{-\frac{rn_0 t}{e-1}} \right)}{rn_0 t (1 - e^{-\frac{d}{L}})} = \frac{1}{e} \quad (21)$$

If we use the data provided by Zhou,⁴ ($\tau = 736$ ns, $d=350$ nm, band gap = 1.55 eV), then r is calculated as $1.23 \times 10^{-9} cm^3/s$. The decay curves from the experiment and decay estimated with $r = 1.23 \times 10^{-9} cm^3/s$ are shown in figure 18 left. As this method is an approximation, if we change r to $1.03 \times 10^{-9} cm^3/s$, its fit better, as shown in Figure 18 right.

Decay directly-2

Rewrite the equation 15, the carriers density at x and time t is

$$n(x) = \frac{n_0(x)}{rn_0(x)t + 1}$$

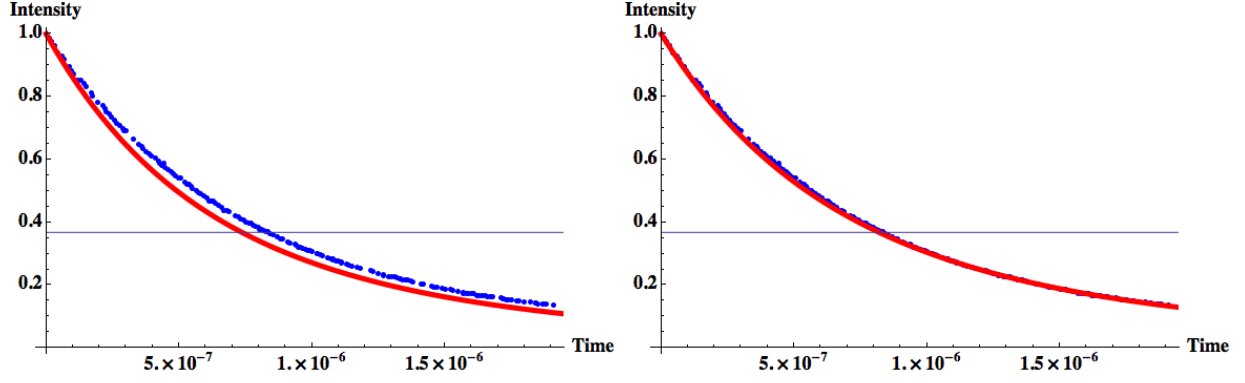


Figure 18: Coefficient estimation. Decay exponentially-1

If the charge carriers is exponentially occupied at $t = 0$, $n_0(x) = \frac{I_0}{L} e^{-\frac{x}{L}}$, then the total charge density at time t is

$$\int_0^d \frac{n_0 e^{-\frac{x}{L}}}{n_0 r t e^{-\frac{x}{L}} + 1} dx$$

$$= \frac{-L \log(e^{d/L} + n_0 r t) + d + L \log(n_0 r t + 1)}{r t}$$

The initial density is $\int_0^d n_0 e^{-\frac{x}{L}} dx$

$$\frac{-L \log(e^{d/L} + n_0 r t) + d + L \log(n_0 r t + 1)}{n_0 r t \left(L - L e^{-\frac{d}{L}} \right)} = \frac{1}{e} \quad (22)$$

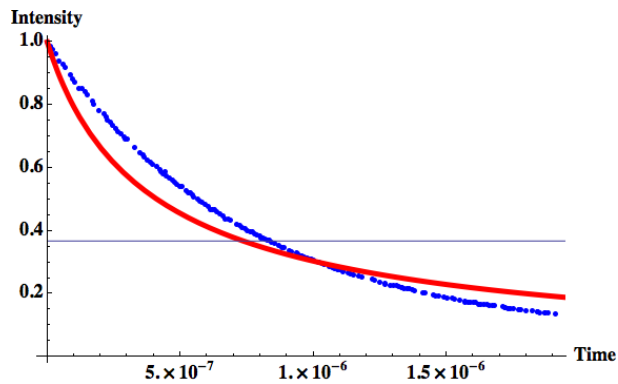


Figure 19: Coefficient estimation. Decay directly-2

If we use the data provided by Zhou,⁴ ($\tau = 736$ ns, $d=350$ nm, band gap = 1.55 eV),

then r is calculated as $1.33 \times 10^{-9} \text{cm}^3/\text{s}$. The decay curves from the experiment and decay estimated with $r = 1.33 \times 10^{-9} \text{cm}^3/\text{s}$ are shown in Figure 19. Due to its poor agreement, this method is abandoned.

References

- (1) Press, W.; Teukolsky, S.; Vetterling, W.; Flannery, B. *Cambridge Uni*, 2nd ed.; 1992.
- (2) Xing, G.; Mathews, N.; Sun, S.; Lim, S. S.; Lam, Y. M.; Grätzel, M.; Mhaisalkar, S.; Sum, T. C.; Gratzel, M. *Science* **2013**, *342*, 344–347.
- (3) Zhou, Y.; Huang, F.; Cheng, Y.-B.; Gray-Weale, A. *Phys. Chem. Chem. Phys.* **2015**, *17*, 22604–22615.
- (4) Zhou, H.; Chen, Q.; Li, G.; Luo, S.; Song, T.-b.; Duan, H.-S.; Hong, Z.; You, J.; Liu, Y.; Yang, Y. *Science* **2014**, *345*, 542–546.
- (5) Stranks, S. D.; Eperon, G. E.; Grancini, G.; Menelaou, C.; Alcocer, M. J. P.; Leijtens, T.; Herz, L. M.; Petrozza, A.; Snaith, H. J. *Science* **2013**, *342*, 341–4.
- (6) Ogiya, K.; Lv, C.; Suzuki, A.; Sahnoun, R.; Koyama, M.; Tsuboi, H.; Hatakeyama, N.; Endou, A.; Takaba, H.; Kubo, M.; Del Carpio, C. A.; Miyamoto, A. *Jpn. J. Appl. Phys.* **2008**, *47*, 3010–3014.
- (7) Onodera, M.; Ogiya, K.; Suzuki, A.; Tsuboi, H.; Hatakeyama, N.; Endou, A.; Takaba, H.; Kubo, M.; Miyamoto, A. *Jpn. J. Appl. Phys.* **2010**, *49*, 04DP10.